

WORLDLINE APPROACH TO THE CASIMIR EFFECT

L. MOYAERTS, K. LANGFELD

*Institut für Theoretische Physik, Universität Tübingen
D-72076 Tübingen, Germany*

H. GIES

*Institut für Theoretische Physik, Universität Heidelberg
D-69120 Heidelberg, Germany*

We present a new method to compute quantum energies in presence of a background field. The method is based on the string-inspired worldline approach to quantum field theory and its numerical realization with Monte-Carlo techniques. Our procedure is applied to the study of the Casimir force between rigid bodies induced by a fluctuating real scalar field. We test our method with the classic parallel-plate configuration and study curvature effects quantitatively for the sphere-plate configuration. The numerical estimates are compared with the “proximity force approximation”. Sizable curvature effects are found for a distance-to-curvature-radius ratio of $a/R > 0.02$.

1 Introduction

This work is based on the formulation of the Casimir effect in the framework of a renormalizable quantum field theory. The Casimir energy is accessed via the quantum effective action expressed in the string-inspired worldline approach to quantum field theory¹. Calculations are performed using a recently developed numerical method to compute quantum energies in presence of a background field², which has already proved to be useful in the study of fermion-induced effects of magnetic interfaces³. In the next section, we derive the expression of the effective action on the worldline, define the Casimir energy and describe briefly the renormalization program. Section 3 is devoted to the loop cloud method, our numerical implementation of worldline calculations. Finally, we focus in section 4 on the study of Casimir forces between rigid bodies for the classic parallel-plate configuration, which serves as test for the method, as well as for the experimentally relevant sphere-plate configuration. Curvature effects are investigated and a comparison with the proximity force approximation is performed.

2 Worldline formalism

The embedding of the Casimir effect in quantum field theory, which is used in this approach and other contributions to this conference⁴, is an alternative to the standard approach of imposing *ab initio* boundary conditions on the fluctuating field. By contrast, the quantum field theoretic approach permits a realistic modeling of the interactions with the physical boundary and a careful

study of the Casimir energy in the limiting case where boundary conditions are satisfied ⁵.

We focus in this work on the Casimir effect induced by a fluctuating real scalar field. The starting point is given by the field theoretic lagrangian

$$\mathcal{L} = \frac{1}{2}\partial_\mu\phi\partial_\mu\phi + \frac{1}{2}m^2\phi^2 + \frac{1}{2}V(x)\phi^2. \quad (1)$$

Here we work in $D = d + 1$ Euclidean spacetime dimensions, i.e. d space dimensions. The interplay between the fluctuating field and the boundary matter is taken into account by the interaction term $V(x)\phi^2$ where the potential $V(x)$ models the physical properties of the Casimir interface. The complete unrenormalized quantum effective action for V is

$$\Gamma[V] = \frac{1}{2}\text{Tr} \ln \frac{-\partial^2 + m^2 + V(x)}{-\partial^2 + m^2}. \quad (2)$$

The worldline representation of $\Gamma[V]$ is obtained ⁶ by (i) introducing the proptime representation of the functional logarithm with UV regularization (e.g. a cutoff Λ at the lower bound of the proptime integral), (ii) performing the trace *in configuration space* $\text{Tr}[\hat{\mathcal{O}}] \rightarrow \int d^D x \langle x | \hat{\mathcal{O}} | x \rangle$ and (iii) interpreting the matrix element as a quantum mechanical transition amplitude expressed by a *Feynman path integral*. The final expression reads

$$\Gamma[V] = -\frac{1}{2(4\pi)^{D/2}} \int_{1/\Lambda^2}^{\infty} \frac{dT}{T^{D/2+1}} e^{-m^2 T} \int d^D x_{\text{CM}} [\langle W_V[T, x(\tau)] \rangle_x - 1], \quad (3)$$

where the expectation value is defined by

$$\langle W_V[T, x(\tau)] \rangle_x := \frac{\int_{x(0)=x(T)} \mathcal{D}x(\tau) e^{-\int_0^T d\tau V(x_{\text{CM}}+x(\tau))} e^{-\int_0^T d\tau \frac{\dot{x}^2}{4}}}{\int_{x(0)=x(T)} \mathcal{D}x(\tau) e^{-\int_0^T d\tau \frac{\dot{x}^2}{4}}}. \quad (4)$$

This expression is the central piece of the worldline approach to quantum field theory. From Eq.(3), we see that the computation of the effective action corresponding to the theory (1) with potential V is based on the average of the holonomy factor $W_V[T, x(\tau)]$ over all *worldlines* $x(\tau)$ which are parametrized by the proptime $\tau \in [0, T]$ and closed, $x(0) = x(T)$, due to the tracing operation in Eq.(2). In Eq.(3), all worldline loops have a common center of mass x_{CM} , which implies $\int_0^T d\tau x_\mu(\tau) = 0$.

In this work, we concentrate exclusively on static Casimir configurations, i.e. the modeling potential

$$V(x) = V(\mathbf{x})$$

is time independent. In this case, the proptime integrand itself does not depend on time and the time integration can be carry out trivially,

$\int dx_{\text{CM}}^0 = L_{x_0}$, where L_{x_0} denotes the “volume” in time direction. We define the (unrenormalized) Casimir energy as

$$\mathcal{E}_V = \Gamma[V]/L_{x_0}. \quad (5)$$

The effective action as given in Eq.(3) is an alternative formulation of the quantum field theory defined from (1). For this reason, the divergence structure of the unrenormalized effective action on the worldline can be expressed in the language of conventional Feynman diagrams. This is done by expanding the proptime integrand in Eq.(3) for small values of T :

$$\int d^D x \langle W_V[T, x(\tau)] - 1 \rangle_x = -T \int d^D x V(x) + \frac{T^2}{2} \int d^D x V(x)^2 + \mathcal{O}(T^3), \quad (6)$$

which should be read together with the proptime factor $1/T^{D/2+1}$ of Eq.(3). For $D > 2$, the first term is divergent and can always be eliminated by using the “no-tadpole” renormalization scheme. The second term is divergent for $D \geq 4$ and contributes to the one-loop diagram containing two insertions of the potential. Standard renormalization provides us with a counter term $\sim \int dx V^2$ subject to a physically chosen renormalization condition such that the divergence arising from the T^2 is canceled and which fixes the physical value of the renormalized operator $\sim V^2$.

This procedure permits to handle these divergences which have a clear field theoretic origin. Moreover further divergences may arise from the *modeling* of the Casimir configuration, i.e. from the potential V itself. These divergences occur when the potential is tuned to take some limiting form $V \rightarrow V_{\text{cr}}$ correspondingly to some convenient assumptions (ideal cases), $\Gamma[V \rightarrow V_{\text{cr}}] \rightarrow \infty$, and may not be removed in a physically meaningful way. The relevant question then is as to whether physical observables are affected by these divergences or not. If not, the problem can possibly be bypassed.

3 Loop Cloud Method

As it is clear from Eq.(3), the main task to be performed is the average (4) over the ensemble of all closed worldlines $x(\tau)$ centered upon a given point x_{CM} . The idea of the loop cloud method is to perform this expectation value by generating the loop ensemble in a numerical way². It is evident that we can generate neither the whole loop ensemble, which is infinite, nor an arbitrarily big amount of loops, for clear reasons of computational time. We will adopt a strategy which is widely used in statistical physics, namely the selection among the ensemble of all loops of the relevant configurations contributing to the loop average. These are generated according to the Gaussian loop distribution $p_{\text{loop}}[T, x(\tau)] \simeq e^{-\int_0^T d\tau \frac{\dot{x}^2}{4}}$. Generating an ensemble of N_{lp} such

loops $\{x(\tau)|_i, i = 1, \dots, N_{\text{lp}}\}$, the expectation value (4) is approximated by

$$\langle W_V[T, x(\tau)] \rangle_x \simeq \frac{1}{N_{\text{lp}}} \sum_{i=1}^{N_{\text{lp}}} W_V[T, x(\tau)|_i]. \quad (7)$$

The numerical burden is moreover dramatically reduced if we rescale the loops $x_\mu(\tau)$ in such a way that the distribution p_{loop} becomes T -independent. Let us consider the following rescaling transformations:

$$\tau \in [0, T] \rightarrow t := \frac{\tau}{T} \in [0, 1], \quad x(\tau) \rightarrow y(t) := \frac{x(tT)}{\sqrt{T}}.$$

The proptime integral appearing in the loop distribution becomes

$$\int_0^T d\tau \dot{x}^2(\tau) \rightarrow \int_0^1 dt \dot{y}^2(t)$$

where the T -dependence has indeed disappeared. The numerical task is then reduced to the all-at-once generation¹ of an ensemble of y -loops, which are called *unit loops*. The evaluation of the expectation value (7) for a given value of T consists then simply in the rescaling of all members of the unit loop ensemble $x(\tau) = \sqrt{T}y(\tau/T)$ before the sum (7) is performed. It is also obvious that the concept of continuous loops has to be abandoned. In the simulations a loop is defined by a collection of N_{ppl} points, corresponding to the discretization of the proptime interval $[0, T]$:

$$x(\tau) \rightarrow \{x_0 = x(\tau_0), x_1 = x(\tau_1), \dots, x_{N_{\text{ppl}}-1} = x(\tau_{N_{\text{ppl}}-1}), x_{N_{\text{ppl}}} = x_0\}.$$

Let us point out that this discretization is not to be mistaken for a spacetime discretization. Every point x_i can move freely in continuous spacetime.

The loop cloud method is developed independently of the background potential. This implies in particular that the Casimir effect can be studied numerically for arbitrary geometries and independently of the degree of symmetry of the physical boundaries. This permits us to go beyond the geometry restrictions required by the 'proximity force approximation' (PFA)^{7,8}, which is the standard analytical approach to non trivial geometric configurations. Beyond this, the method does not require perfect geometries and perfect surfaces but can, for instance, facilitate the study of corrugated surfaces⁹.

4 Casimir forces between rigid bodies

In this work, we model the physical boundaries by a potential of the form

$$V(\mathbf{x}) = \lambda f(\mathbf{x}),$$

where $f(\mathbf{x})$ describes the geometry of the Casimir configuration and $\lambda > 0$ is the strength of the field-matter interaction. It can roughly be viewed as a plasma frequency of the boundary matter: for fluctuations with frequency

$\omega \gg \lambda$, the Casimir boundaries become transparent. Two types of limits can be taken regarding this parametrization:

$$f(\mathbf{x}) \rightarrow \int_{\Sigma} d\sigma \delta^d(\mathbf{x} - \mathbf{x}_{\sigma}) \text{ (sharp potential limit),} \quad (8)$$

$$\lambda \rightarrow \infty \quad \text{(strong coupling limit).} \quad (9)$$

Here Σ represents the geometry of the Casimir configuration and denotes a $d - 1$ dimensional surface, generally disconnected (e.g. two separated plates, $\Sigma = S_1 + S_2$). The first limit idealizes the plate to be infinitely thin. The second limit imposes the *Dirichlet boundary condition*, implying that all modes have to vanish on Σ . Together they correspond to the case of *ab initio* boundary conditions of the standard approach. These limits are unfortunately spoiled by the occurrence of a divergence in the Casimir energy which cannot be removed by the standard field theoretic renormalization procedure. However, this problem can be bypassed if we consider instead the Casimir *force* acting on the rigid bodies. The force is defined by

$$F_{\text{Cas}}(a) = -\frac{\partial}{\partial a} E_{\text{Cas}}(a)$$

where a denotes the distance between the boundaries. This definition gives us a certain freedom of the choice of the *Casimir interaction energy* $E_{\text{Cas}}(a)$. For a Casimir configuration of two rigid bodies whose surfaces are denoted by S_1 and S_2 , we define the interaction energy as

$$E_{\text{Cas}}(a) = \mathcal{E}_{V_{1+2}}(a) - \mathcal{E}_{V_1} - \mathcal{E}_{V_2} \quad (10)$$

where $\mathcal{E}_{V_{1+2}}$, \mathcal{E}_{V_1} and \mathcal{E}_{V_2} are the energies (5) with the potentials V_{1+2} , V_1 and V_2 given in the limiting form (8) where $\Sigma = S_1 \cup S_2$, $\Sigma = S_1$ and $\Sigma = S_2$, respectively. The first term depends on the distance a and contributes to the Casimir force. Since the remaining terms do not depend on a , the way there are chosen has no influence on the Casimir force. In the present case, they are chosen in such a way that $E_{\text{Cas}}(a)$ is rendered finite by subtracting each Casimir energy of the single bodies.

4.1 A benchmark test: the parallel plates revisited

Casimir forces can be analytically computed only for a small number of rigid-body geometries among which there is the parallel-plate configuration. Comparing our numerical estimates with the analytically known result¹⁰, the agreement is very satisfying in all regimes of scalar mass m , coupling λ and distance a , see Fig.1, right panel. Moreover, we have found that our algorithm is scalable: if higher precision is required, only the parameters of the loop ensemble, points per loop N_{ppl} which controls the systematic error induced by the loop discretization and number of loops N_{lp} which controls the approximation of the loop average (4) by the sum (7), have to be adjusted, as seen in Fig.1, left panel.

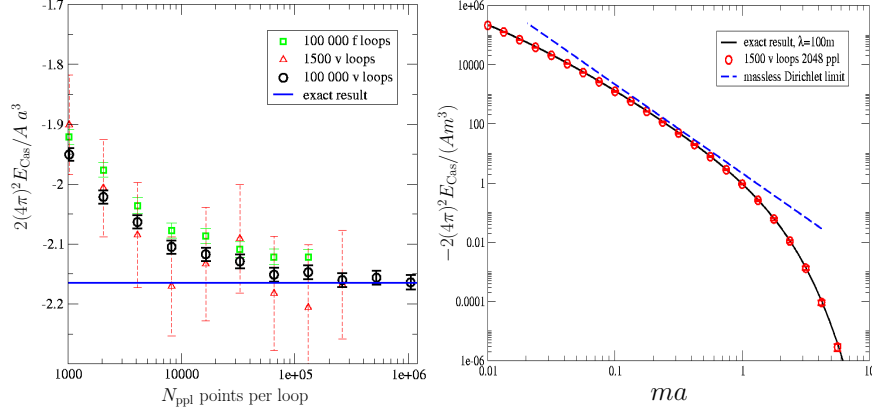


Figure 1. Numerical estimate of the interaction Casimir energy per unit area of the parallel-plate configuration for various loop ensembles as a function of the number of points per loop N_{ppl} (left panel). Numerical estimates vs. analytical results as a function of the dimensionless quantity ma , $\lambda = 100m$ (right panel).

4.2 Beyond the PFA: the sphere-plate configuration

We study the experimentally relevant sphere-plate configuration and confront our numerical estimates with the results provided by the proximity force approximation (PFA). Due to the assumptions on which the PFA is based, i.e. dropping of non-local curvature effects, this approach is expected to give reasonable results only if the typical curvature radii of the surfaces elements is large compared to the element distance. Beside its physical interest, the sphere-plate configuration with its relatively simple geometry provides us with a beautiful illustration of the loop cloud machinery. As illustrated in Fig.2, the main feature of the sphere-plate physics, i.e. curvature effects, can be understood qualitatively simply by thinking in terms of loops. On the one hand, the energy density at a point x_0 is obtained by performing averages over loop clouds centered on x_0 . On the other hand, it can be shown that the energy density is proportional to the number of loops piercing both physical boundaries. With these two statements only, Fig.(2) can be qualitatively understood. The effect of the increasing curvature of one of the boundaries is the decrease of contributing loops near the plate, implying the decrease of the Casimir energy in this region.

Let us finally consider the complete interaction Casimir energy for the sphere-plate configuration as a function of the sphere-plate distance a (we express all dimensionful quantities as a function of the sphere radius R). In Fig. 3, we plot our numerical results in the range $a/R \simeq \mathcal{O}(0.001 \dots 10)$. Since the energy varies over a wide range of scales, already small loop ensembles with rather large errors suffice for a satisfactory estimate (the error bars of

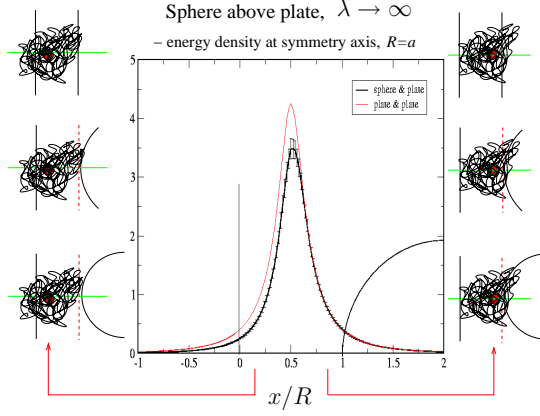


Figure 2. Interaction Casimir energy density along the symmetry axis (x axis) for the sphere-plate configuration in comparison to the parallel-plate case. Close to the sphere, the worldline loops do not “see” the curvature; but at larger distances, curvature effects enter the energy density. For illustration, the sphere-plate geometry is also sketched (thin black lines).

an ensemble of 1500 loops with 4000 ppl cannot be resolved in Fig. 3). Let us compare our numerical estimate with the proximity force approximation with radial distance measurements: using the plate surface as the integration domain for the PFA, we obtain the solid line in Fig. 3 (PFA, plate-based), corresponding to a “no-curvature” approximation. As expected, the PFA approximation agrees with our numerical result for small distances (large sphere radius). Sizable deviations from the PFA approximation of the order of a few percent occur for $a/R \simeq 0.02$ and larger. Here, the curvature-neglecting approximations are clearly no longer valid. This can be read off from the right panel, where the resulting interaction energies are normalized to the numerical result.

5 Conclusion

In this work, we have developed a new numerical method to compute quantum energies in presence of a background field. The algorithm is constructed independently of the background, which opens a wide range of applicability of the procedure. In the context of the Casimir effect, arbitrary geometric configurations can be considered. We focused in this work on the Casimir forces induced on rigid bodies by the fluctuations of a real scalar field. The method was tested by comparing our numerics with the analytical results in the classic parallel-plates configuration and confronted with the results provided by the proximity force approximation in the sphere-plate configuration.

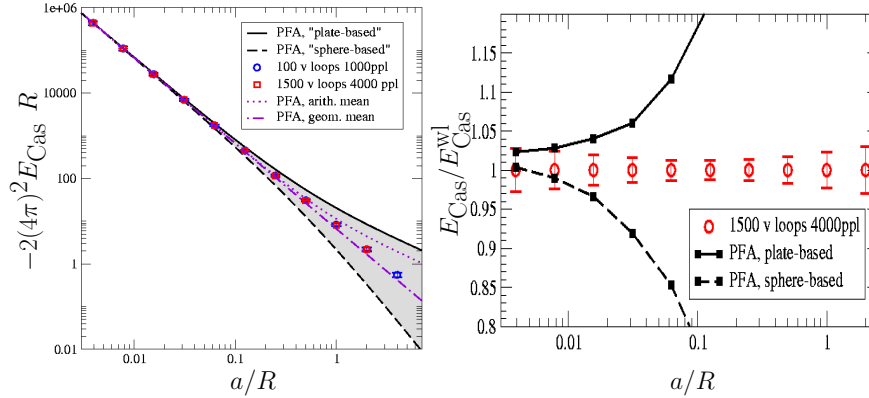


Figure 3. **Left panel** Logarithmic plot of the interaction Casimir energy for the sphere-plate configuration. For small separations/large spheres, $a/R < 0.02$, the proximity force approximation (PFA) approximates the numerical estimate well; but for larger a/R , curvature effects are not properly taken into account. The PFA becomes ambiguous for larger a/R , owing to possible different choices of the integration domain in the PFA. A geometric mean (dotted-dashed line) of the limiting cases shows reasonable agreement with the numerical result. **Right panel** Interaction Casimir energies normalized to the numerical result. For $a/R > 0.02$, the fluctuation-induced curvature effects occur at the percent level.

We have been able to study the usually neglected nonlocal curvature effects which become sizable for a distance-to-curvature-radius ratio of $a/R > 0.02$. Some generalizations to more realistic configurations are straightforward: finite temperature effects, surface roughness and corrugation. Let us finally note that the implementation of worldline numerics for the Casimir effect due to a fluctuating electromagnetic field has still to be worked out. Here the new ingredient is to find an efficient field theoretic formulation of the interaction of the electromagnetic field with the Casimir boundaries.

Acknowledgments

L.M. is grateful to the organizers of the QFEXT03 meeting in Norman for the stimulating atmosphere of the conference and acknowledges financial support by the Deutsche Forschungsgemeinschaft under contract GRK683. H.G. is supported by the Deutsche Forschungsgemeinschaft under contract Gi 328/1-2.

References

1. H. Gies, K. Langfeld and L. Moyaerts, JHEP **0306** (2003) 018.
2. H. Gies and K. Langfeld, Nucl. Phys. B **613** (2001) 353,
H. Gies and K. Langfeld, Int. J. Mod. Phys. A **17** (2002) 966.

3. K. Langfeld, L. Moyaerts and H. Gies, Nucl. Phys. B **646** (2002) 158.
4. N. Graham, R. L. Jaffe, V. Khemani, M. Quandt, M. Scandurra and H. Weigel, Phys. Lett. B **572** (2003) 196.
5. R. L. Jaffe, arXiv:hep-th/0307014.
6. For a review see C. Schubert, Phys. Rept. **355** (2001) 73.
7. B.V. Derjaguin, I.I. Abrikosova, E.M. Lifshitz, Q.Rev. **10** (1956) 295.
8. J. Blocki, J. Randrup, W.J. Swiatecki, C.F. Tsang, Ann. Phys. (N.Y.) **105** (1977) 427.
9. T. Emig, Europhys. Lett. **62** (2003) 466.
10. M. Bordag, D. Hennig and D. Robaschik, J. Phys. A **25** (1992) 4483.